

LETTER

Subcarrier Block Power Control for Adaptive Downlink OFDM with Frequency Spreading and Equalization

Nam-Su KIM^{†(a)}, Sungho CHO[†], Nonmembers, and Chang-Jun AHN^{††}, Member

SUMMARY In this letter, we propose the transmit power controlled adaptive downlink frequency symbol spreading OFDM (TPC-AMS/FSS-OFDM) system. In the TPC-AMS/FSS-OFDM, each S/P transformed signal is spread by orthogonal spreading codes and combined in the transmitter, so the detected signals obtain the same SINR for each frequency symbol spreading block in the receiver. In this case, we can assign the same modulation level and transmit power for each frequency symbol spreading block for next transmission. Thus, the proposed system not only increases throughput performance but also reduces the total transmit power, FBI and MLI.

key words: subcarrier block power control, frequency symbol spreading, MMSEC

1. Introduction

There has been growing demand for high-data-rate, high-quality multimedia services in wireless communications. For high data rate in wireless communication, orthogonal frequency division multiplexing (OFDM) with adaptive modulation scheme (AMS) is attractive [1]. However, the base station controls the modulation level of each subcarrier, and then, adaptive modulated packets are transmitted from the base station to the mobile station. In this case, the mobile station also requires modulation level information (MLI) to demodulate received packets. Because the MLI is generally transmitted as a data symbol, the throughput is degraded in the downlink of AMS/OFDM, as a result of the MLI transmission. To overcome above-mentioned problems and increase the total throughput, frequency symbol spreading and frequency equalization based on an adaptive downlink OFDM system (AMS/FSS-OFDM) has been proposed [2]. In the AMS/FSS-OFDM, each serial to parallel (S/P) transformed signal is spread by an orthogonal spreading code with length N_{SF} over the N_{SF} subcarriers, and combined in the transmitter. This means that each subcarrier holds several superimposed S/P transformed signals with the same power rate. In this case, we can assign the same modulation level for each frequency symbol spreading block. Recently, subcarrier power controlled OFDM systems are being widely considered for reducing the transmit power [3].

However, subcarrier power controlled OFDM systems require a large feedback information (FBI) to assign a suitable transmit power for each subcarrier. When we consider the power control scheme to AMS/FSS-OFDM, we can assign the same controlled transmit power for each frequency symbol spreading block with the same modulation level. Therefore, the transmit power controlled AMS/FSS-OFDM provides the increased throughput performance with reducing the total transmit power, FBI and MLI. This letter is organized as follows. The power controlled adaptive downlink FSS-OFDM (TPC-AMS/FSS-OFDM) system is described in Sect. 2. In Sect. 3, we describe our simulation results, before giving our conclusions in Sect. 4.

2. TPC-AMS/FSS-OFDM

2.1 Transmitter Structure

The transmitter block diagram of TPC-AMS/FSS-OFDM system is shown in Fig. 1(a). The coded binary information data sequence is modulated by using the adaptive modulation command (AMC), and N_p pilot symbols are appended at the beginning of a sequence. The symbol sequence consists of S/P converted to N_c parallel sequences. The n th parallel sequence is fed into the $(n-1 \bmod N_{SF})$ th subcode processing block of the $\lfloor n/N_{SF} \rfloor$ th frequency symbol spreading block, where N_{SF} is the spreading code length, and $\lfloor x \rfloor$ de-

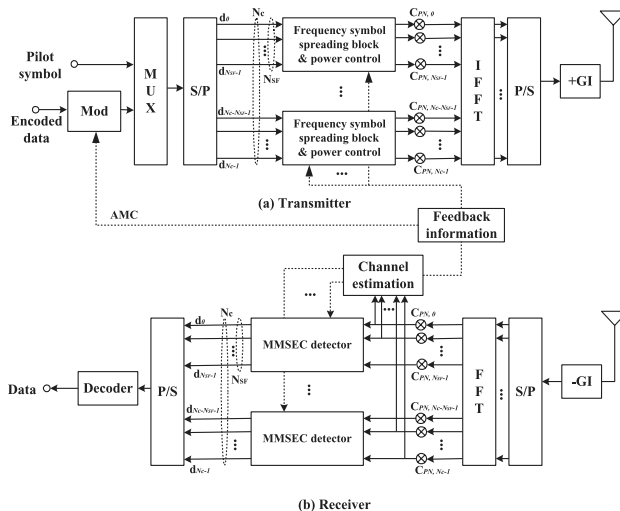


Fig. 1 Proposed transmit power controlled adaptive downlink FSS-OFDM system (TPC-AMS/FSS-OFDM).

Manuscript received December 16, 2005.

Manuscript revised February 28, 2006.

[†]The authors are with the Department of Electronic Engineering, Hanyang University, 17 Haengdang-dong, Seongdong, Seoul, 133-791 Korea.

^{††}The author is with the National Institute of Information and Communication Technology (NICT), Incorporated Administrative Agency, Yokosuka-shi, 239-0847 Japan.

a) E-mail: nskim7@korea.com

DOI: 10.1093/ietcom/e89-b.7.2102

notes the largest integer less than or equal to x . Each parallel sequence fed into the frequency symbol spreading block is copied by the same length of orthogonal spreading code with length N_{SF} . These copied parallel complex sequences are spread by the orthogonal spreading code with N_{SF} and combined. The combined parallel sequences are power controlled by using the feedback information, and then, the resulting combined parallel sequences are also spread by the sequence of a long pseudo-random scrambling code (c_{PN}) in the frequency domain. The transmitting FSS-OFDM signal waveform is obtained by applying an inverse Fourier transform (IFFT). The TPC-AMS/FSS-OFDM transmit signal can be expressed in its equivalent baseband representation as

$$s(t) = \sum_{i=0}^{N_p+N_d-1} g(t-iT) \cdot \left\{ \sqrt{\frac{2S}{N_c}} \sum_{n=0}^{N_c-1} c_{PN}(n) \cdot u(n, i) \cdot \exp[j2\pi(t-iT)n/T_s] \right\}, \quad (1)$$

where T_s is the effective symbol length, S is the power controlled average transmitting power, T is the OFDM symbol length, c_{PN} is a long pseudo-noise (PN) sequence, and $u(n, i)$ is the n th subcarrier of the i th OFDM symbol. The frequency separation between adjacent orthogonal subcarriers is $1/T_s$ and can be expressed by using the n th subcarrier of the i th modulated symbol $d(n, i)$ with $|d(n, i)| = 1$, as

$$u(n, i) = \sum_{k=0}^{N_{SF}-1} c_k(n \bmod N_{SF}) \cdot d[\lfloor n/N_{SF} \rfloor \cdot N_{SF} + k, i], \quad (2)$$

where N_c is the number of subcarriers. In Eq. (1), $g(t)$ is the transmission pulse given by

$$g(t) = \begin{cases} 1 & -T_g \leq t \leq T_s \\ 0 & \text{otherwise.} \end{cases} \quad (3)$$

2.2 Receiver Structure

The receiver structure is illustrated in Fig. 1(b). By applying the FFT operation, the received signal $r(t)$ is resolved into N_c subcarriers. The received signal $r(t)$ in the equivalent baseband representation can be expressed as

$$r(t) = \int_{-\infty}^{\infty} h(\tau, t) s(t-\tau) d\tau + n(t), \quad (4)$$

where $n(t)$ is additive white Gaussian noise (AWGN) with a single sided power spectral density of N_0 . The n th subcarrier $\tilde{r}(n, i)$ is given by

$$\begin{aligned} \tilde{r}(n, i) &= \frac{1}{T_s} \int_{iT}^{iT+T_s} r(t) \exp[-j2\pi(t-iT)n/T_s] dt \\ &= \sqrt{\frac{2S}{N_c}} \sum_{e=0}^{N_c-1} u(e, i) \cdot \frac{1}{T_s} \int_0^{T_s} \exp[j2\pi(e-n) \cdot t/T_s] \cdot \left\{ \int_{-\infty}^{\infty} h(\tau, t+iT) g(t-\tau) \right. \\ &\quad \left. \cdot \exp(-2\pi e\tau/T_s) d\tau \right\} dt + \hat{n}(n, i), \end{aligned} \quad (5)$$

where $\hat{n}(n, i)$ is AWGN noise with zero-mean and a variance of $2N_0/T_s$. Assuming that the maximum τ_l is shorter than the guard interval T_g , the integral with respect to τ becomes, from Eq. (3),

$$\begin{aligned} &\int_{-\infty}^{\infty} h(\tau, t+iT) g(t-\tau) \exp(-j2\pi e\tau/T_s) d\tau \\ &= \int_0^{T_s} h(\tau, t+iT) \exp(-j2\pi e\tau/T_s) d\tau \\ &= H(e/T_s, t+iT). \end{aligned} \quad (6)$$

Assuming that $\epsilon_i(t)$ remains almost constant over the symbol length T ,

$$\epsilon_i(t+iT) \approx \epsilon_i(iT) \quad \text{for } 0 \leq t \leq T, \quad (7)$$

and hence, we have

$$H(n/T_s, t+iT) \approx H(n/T_s, iT) \quad \text{for } 0 \leq t \leq T. \quad (8)$$

As a result, Eq. (5) can be rewritten as

$$\begin{aligned} \tilde{r}(n, i) &\approx \frac{1}{T_s} \sqrt{\frac{2S}{N_c}} \sum_{e=0}^{N_c-1} u(e, i) \cdot \int_0^{T_s} \exp[j2\pi(e-n) \cdot t/T_s] dt + \hat{n}(n, i) \\ &= \sqrt{\frac{2S}{N_c}} H(n/T_s, iT) u(n, i) + \hat{n}(n, i). \end{aligned} \quad (9)$$

Observing Eq. (9), we can see that the received signals have frequency distortion arising from the frequency-selective fading. To reduce this frequency distortion, frequency equalization combining is necessary. The combining weight for the n th subcarrier is denoted by $w(n, i)$. After frequency equalization combining, the received modulated data symbol can be written as

$$\begin{aligned} \tilde{d}(n, i) &= \sum_{k=0}^{N_{SF}-1} \hat{u}[\lfloor n/N_{SF} \rfloor \cdot N_{SF} + k, i] \\ &\quad \cdot c_{n \bmod N_{SF}}^*(k), \end{aligned} \quad (10)$$

where $\{\hat{u}(q+k, i), k=0, 1, \dots, N_{SF}-1\}$ is the weighted component of the n th subcarrier and is given by

$$\begin{aligned} \hat{u}(n, i) &= w(n, i) c_{PN}^*(n) \tilde{r}(n, i) \\ &= \sqrt{\frac{2S}{N_c}} H(n/T_s, iT) u(n, i) c_{PN}^*(n) w(n, i) \\ &\quad + \hat{n}(n, i) c_{PN}^*(n) w(n, i). \end{aligned} \quad (11)$$

2.3 Pilot-Symbol-Assisted Channel Estimation for Frequency Equalization Combining

As indicated by Eq. (9), frequency equalization combining is necessary to reduce the frequency distortion arising from frequency-selective fading. Here, we explain a channel estimation scheme using N_p pilot symbols. The channel response of the n th subcarrier is given by

$$\tilde{H}(n/T_s) = \frac{1}{N_p \sqrt{2P/N_c}} \sum_{i=0}^{N_p-1} \tilde{r}(n, i) \cdot p^*(n, i) \cdot c_{PN}^*(i), \quad (12)$$

where $\{p(n, i), 0 \leq i \leq N_p - 1\}$ and P are the transmitted pilot symbol and the power, respectively. Estimation of the noise power $\tilde{\sigma}$ in each subcarrier component is required for minimum mean square error combining (MMSEC).

$$\tilde{\sigma}_n^2 = \frac{1}{N_p \sqrt{2P/N_c}} \left| \sum_{i=0}^{N_p-1} \tilde{r}(n, i) - \sqrt{2S/N} \cdot \tilde{H}(n/T_s) \right|^2, \quad (13)$$

for $N_p - 1 > 1$. Assuming that the noise power is identical for all subcarriers, i.e., $\tilde{\sigma}_n^2 = \sigma^2$ is estimated using

$$\tilde{\sigma}^2 = \frac{1}{N_c} \sum_{n=0}^{N_c-1} \tilde{\sigma}_n^2. \quad (14)$$

The MMSEC weight $\omega_{MMSEC}(n, i)$ is given by

$$\omega_{MMSEC}(n, i) = \frac{\sqrt{\frac{2S}{N_c}} \cdot \tilde{H}(n/T_s)}{\left| \sqrt{\frac{2S}{N_c}} \cdot \tilde{H}(n/T_s) \right|^2 + 2\tilde{\sigma}^2}. \quad (15)$$

From Eqs. (10), (11) and (14), we can calculate the signal interference to noise ratio (SINR) of each frequency spreading block for generating the FBI. From Fig. 2, the proposed system obtains the same SINR of each frequency symbol spreading block. Therefore, we can easily assign the modulation level and transmit power.

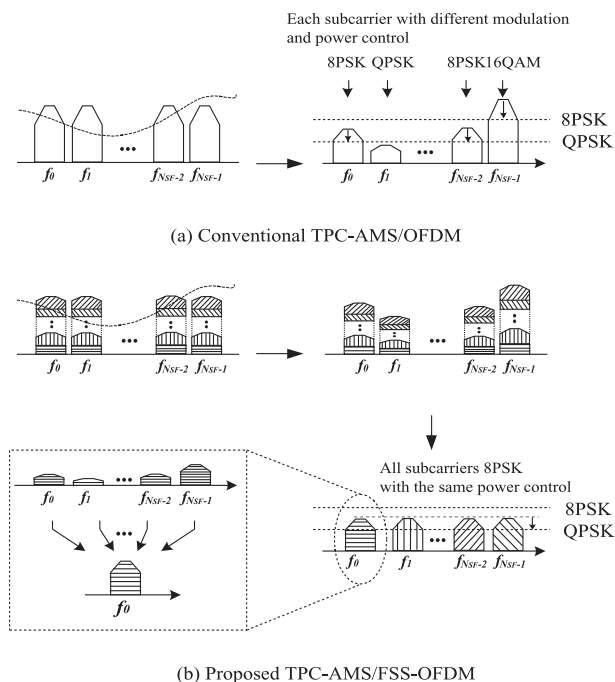


Fig. 2 Basic concept of the proposed TPC-AMS/FSS-OFDM system.

3. Computer Simulation Results

Figure 1 shows the simulation model that we used for power controlled adaptive OFDM with $N_c = 64$ subcarriers. The guard interval time is $1.2 \mu\text{s}$ and the effective symbol duration is $4.5 \mu\text{s}$, respectively. On the transmitter side, the data stream is encoded. Here, convolutional codes (rate $R = 1/2$, constraint length $K = 7$) are applied. The goal of the adaptive modulation is to maximize the throughput to maintain the acceptable BER. In this evaluation, we set the target BER of 10^{-5} . The channel model that is a seven-ray exponential decaying multipath model and each path complies with Rayleigh fading, and a path separation $T_{path} = 140 \text{ nsec}$. The maximum Doppler frequency is assumed as 10 Hz . In the transmitter, each signal is spread by an orthogonal spreading code, so that each signal can be detected by using orthogonal spreading codes. However, orthogonality among different spreading codes can not be achieved because of the frequency-selective fading. Hence, a frequency equalization combining technique is necessary in order to restore orthogonality. In this simulation, we consider the MMSEC scheme as an equalization scheme. These equalized signals are coherently demodulated according to Eq. (10). A packet consists of 64 subcarriers and 22 OFDM symbols (number of pilot signals: $N_p = 2$; number of data: $N_d = 20$).

Figure 3 shows the BER for uncoded and convolutionally coded FSS-OFDM with MMSEC and $N_{SF}=2, 16$, and 64 , and QPSK, at a Doppler frequency of 10 Hz . With increasing N_{SF} , the BER for uncoded FSS-OFDM can be improved, because uncoded FSS-OFDM can achieve frequency diversity. In the case of short N_{SF} , consecutive subcarriers are strongly correlated, so the frequency diversity is poor. However, for large N_{SF} , the spreading bandwidth is wider than the coherence bandwidth. For this reason, uncoded FSS-OFDM with large N_{SF} achieves greater frequency diversity. However, with FEC and interleaving, the

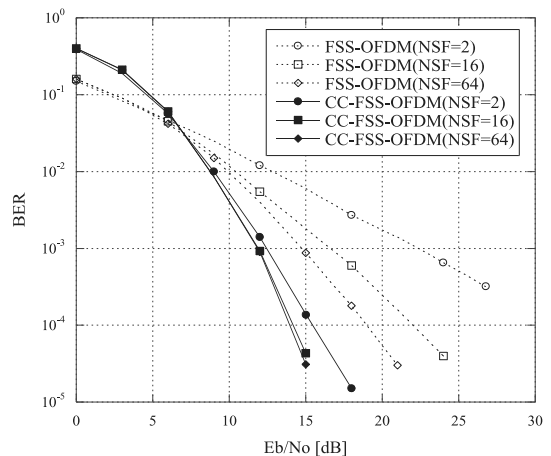


Fig. 3 BER for uncoded and convolutionally coded FSS-OFDM with MMSEC for various cases of N_{SF} , including $N_{SF}=2, 16$, and 64 , and QPSK, at a Doppler frequency of 10 Hz .

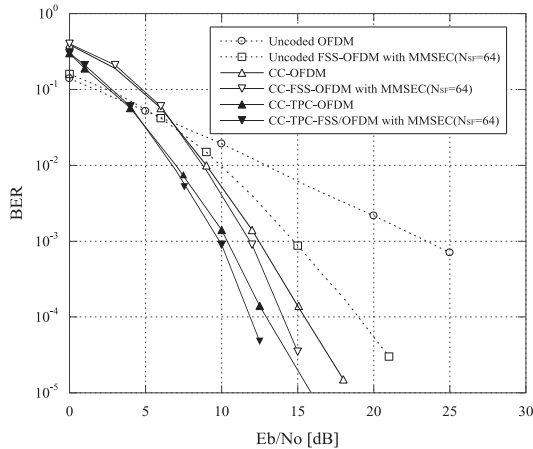


Fig. 4 BER of uncoded and convolutionally coded OFDM and TPC-OFDM, FSS-OFDM with MMSEC, and TPC-FSS/OFDM with MMSEC, for QPSK at a Doppler frequency of 10 Hz.

BERs in the case of different N_{SF} shows approximately the same performance. This is because utilizing FEC and interleaving combination enables full frequency diversity.

Figure 4 shows the BER of uncoded and convolutionally coded OFDM and TPC-OFDM, FSS-OFDM with MMSEC, and TPC-FSS/OFDM with MMSEC for the case of $N_{SF} = 64$ and QPSK, at a Doppler frequency of 10 Hz. The MMSEC scheme provides better BER than that of the conventional OFDM, since it uses all subcarriers and minimizes the power loss while suppressing the noise enhancement. Moreover, TPC-AMS/OFDM and TPC-FSS/OFDM system can reduce the redundant transmit power, so CC-TPC-FSS/OFDM shows the best BER with the reduced transmit E_b/N_o .

Figure 5 shows the throughput for fixed 16QAM, the conventional AMS/OFDM and TPC-AMS/OFDM with MLI on data, AMS/FSS-OFDM with MMSEC, and TPC-AMS/FSS-OFDM with MMSEC at a Doppler frequency of 10 Hz. In an AMS, we used the modulation schemes as QPSK and 16QAM. From Fig. 2, it can be observed that AMS/FSS-OFDM and TPC-AMS/FSS-OFDM systems require only one SINR as FBI for setting a suitable modulation, as compared with the conventional AMS/OFDM and TPC-AMS/OFDM systems. Due to one piece of FBI, the MLI is also required only one piece. Therefore, the throughput performance of AMS/FSS-OFDM and TPC-AMS/FSS-OFDM systems are better than those of the conventional AMS/OFDM and TPC-AMS/OFDM systems. This is because the conventional AMS/OFDM and TPC-AMS/OFDM systems transmit the MLI on data, so the total throughputs are worse than those of the AMS/FSS-OFDM and TPC-AMS/FSS-OFDM systems. Moreover, TPC-AMS/OFDM and TPC-AMS/FSS-OFDM systems reduce the redundant transmit power, so the throughput of TPC-AMS/OFDM and TPC-AMS/FSS-OFDM achieve better than those of

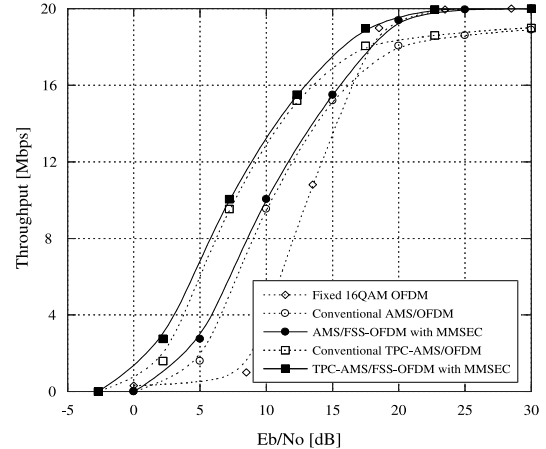


Fig. 5 Throughput of the fixed 16QAM, the conventional AMS/OFDM and TPC-AMS/OFDM with MLI on data, AMS/FSS-OFDM with MMSEC, and TPC-AMS/FSS-OFDM with MMSEC at a Doppler frequency of 10 Hz.

the AMS/FSS-OFDM and TPC-AMS/FSS-OFDM systems with the reduced transmit E_b/N_o .

4. Conclusion

In this letter, we proposed the transmit power controlled adaptive downlink FSS-OFDM (TPC-AMS/FSS-OFDM) system. In the proposed system, each subcarrier signal holds several superimposed signals with the same power rate. Therefore, the detected signals obtain the same SINR for each frequency symbol spreading block. As a result, we can easily assign the same modulation level and the controlled transmit power for each frequency spreading block. The proposed system achieves the better throughput than those of the conventional AMS/OFDM and AMS/FSS-OFDM with reducing the total transmit power.

Acknowledgment

This work was supported by HY-SDR Research Center at Hanyang University, Seoul, Korea, under the ITRC program of MIC, Korea.

References

- [1] T. Keller, T.H. Liew, and L. Hanzo, "Adaptive modulation techniques for duplex OFDM transmission," IEEE Trans. Veh. Technol., vol.49, no.5, pp.1893–1904, Sept. 2000.
- [2] C. Ahn, H. Harada, and Y. Kamio, "Superimposed frequency symbol based adaptive downlink OFDM with frequency spreading and equalization," IEICE Trans. Commun., vol.E89-B, no.2, pp.500–508, Feb. 2006.
- [3] H. Kang, W. Hwang, and K. Kim, "OFDM systems with subchannel power control under the two-ray multipath channel communications," Proc. ICC 2001, vol.6, pp.1856–1860, June 2001.